

PAPER View Article Online
View Journal | View Issue



Cite this: Phys. Chem. Chem. Phys., 2025, 27, 18907

Received 28th July 2025, Accepted 18th August 2025

DOI: 10.1039/d5cp02871j

rsc.li/pccp

Kinetics of the reaction of CF₃CHO with OH between 204 K and 361 K

Fabienne Baumann, **D** Christin Fernholz, **D** Jos Lelieveld and John N. Crowley **D**

Trifluoroacetaldehyde (CF₃CHO) is formed in the atmosphere by the oxidation of a number of fluorinated, organic compounds of anthropogenic origin. The reaction of CF₃CHO with the OH radical is a potential source of atmospheric trifluoroacetic acid (TFA) which is a highly persistent, water-soluble compound that may accumulate in aquatic ecosystems and for which uncertainty about its sources, fate, and potential ecological impact persists. In light of growing concerns about the impact of TFA, we present the first study of the temperature dependence of the rate coefficient for the title reaction over the atmospherically relevant temperature range of 204 K to 361 K. Rate coefficients were determined using pulsed laser photolysis-pulsed laser induced fluorescence (PLP-PLIF) and direct concentration measurements via Fourier Transform Infrared (FTIR) spectroscopy, as well as relative rate experiments in an atmospheric simulation chamber using ethane (C₂H₆) as a reference compound. The rate coefficient (k_1) obtained with PLP-PLIF at room temperature is (5.8 \pm 0.5) \times 10⁻¹³ cm³ molecule⁻¹ s⁻¹. The temperature dependence is described by the expression $k_1(7) = (3.8 \pm 0.2) \times 10^{-13} \times (7/300)^2 \times ($ $\exp[(131 \pm 16)/T]$. The relative-rate experiments showed that the rate coefficient obtained can be significantly biased by reactions of the CF_3O radical with CF_3CHO and/or C_2H_6 and also reactions of CF_3CHO with HO_2 . Based on the expression of k_1 given above, the lifetime of CF_3CHO with respect to reaction with the OH radical varies from 22 days at the surface ($T \sim 300$ K) to 30 days in the upper troposphere ($T \sim 220 \text{ K}$).

1. Introduction

Fluorinated chemicals are produced at a worldwide annual rate of multiple million tons, with a rising trend. Owing to their chemical stability and unique physicochemical properties, 8 they are widely used as refrigerants, propellants, specialty solvents, and high-performance lubricants. It is estimated that $\sim 20\%$ of marketed drugs and ~50% of agrichemicals contain at least one F-atom underlining their importance. 9,10 The generation and usage of fluorinated trace gases including hydrochlorofluorocarbons (HCFCs), hydrofluorocarbons (HFCs), fluorotelomer alcohols and hydrofluoroolefins (HFOs)11-13 results in their release to the atmosphere where they may undergo chemical transformation. While HCFCs and HFCs are long-lived (up to decades) and are transported to the stratosphere, HFOs have lifetimes of the order of days to weeks and are degraded in the lower atmosphere (troposphere). HFOs are of topical interest as they are gaining importance as replacements for traditional refrigerants such as chlorofluorocarbons (CFCs) and hydrofluorocarbons (HFCs)14,15 and are now widely used in a variety of industrial applications, including refrigerants, foam blowing agents and propellants in medical devices. 16-18

Fluorinated chemicals have come under scrutiny owing to their potential risk to the environment as greenhouse gases or precursors to toxic and persistent chemicals. CF₃CHO, the object of this study, is one of the products that can result from the breakdown of some fluorinated chemicals in the atmosphere.

The atmospheric degradation of CF_3CHO proceeds via both photolysis and reaction with OH radicals. Based on the available literature, photolysis is expected to contribute $\sim 80\%$ and reaction with OH $\sim 20\%$. However, there is considerable uncertainty associated with the relative contribution of these loss pathways at *e.g.* different altitudes, as temperature-dependent rate coefficients for (R1) or temperature dependent quantum yields for (R2) have not been published (IUPAC, 2025). The reaction with OH is thought to proceed entirely via abstraction of the aldehydic H-atom to generate the trifluoro acetyl radical (CF₃CO) as written in (R1). The predominant products of photodissociation at actinic wavelengths ($\lambda > 300$ nm) are CF₃ and HCO (R2).

$$CF_3CHO + OH \rightarrow CF_3CO + H_2O$$
 (R1)

$$CF_3CHO + h\nu \rightarrow CF_3 + HCO$$
 (R2)

Max-Planck-Institute for Chemistry, Division of Atmospheric Chemistry, 55128 Mainz, Germany. E-mail: fabienne.baumann@mpic.de, john.crowley@mpic.de The CF₃CO product of (R1), will react with O₂ in air to form the CF₃C(O)O₂ radical (R3), which, *via* subsequent reaction with atmospheric peroxy radicals or reactive nitrogen trace-gases represents a pathway to the formation of stable and semi-stable trace-gases such as CF₃C(O)OH (TFA, (R4a)), CF₃C(O)OOH (trifluoroperacetic acid, (R4b)) and CF₃C(O)O₂NO₂ (trifluoroperoxyacetyl nitric anhydride, FPAN, (R5)).⁵

$$CF_3CO + O_2 + M \rightarrow CF_3C(O)O_2 + M$$
 (R3)

$$CF_3C(O)O_2 + HO_2 \rightarrow CF_3C(O)OH + O_3$$
 (R4a)

$$\rightarrow$$
 CF₃C(O)OOH + O₂ (R4b)

$$\rightarrow$$
 CF₃CO₂ + O₂ + OH (R4c)

$$CF_3C(O)O_2 + NO_2 + M \rightarrow CF_3C(O)O_2NO_2 + M$$
 (R5)

Thus, while the photolysis of CF₃CHO leads to radical fragments that further degrade to *e.g.* CO and F₂CO, reaction with OH maintains the C-2 chain and can thus result in the formation of TFA which is a highly persistent, water-soluble compound that is primarily removed from the atmosphere through wet deposition.²⁰ TFA accumulates in aquatic ecosystems, particularly in oceans and terminal basins, with no known significant degradation pathway.⁶ Although current and predicted environmental concentrations are well below toxic thresholds for aquatic life, debates and uncertainties about the sources, fate, and potential ecological impact of TFA persist.⁷ The formation of FPAN in (R5) may also represent a chemical pathway to TFA *via* hydrolysis on aqueous hydrometeors or wet-surfaces or even *via* reaction with water vapour.²¹

Several experimental studies of the reaction of CF₃CHO with the OH radical have been published and these have been summarised and evaluated by the IUPAC panel which, in the absence of published, temperature-dependent rate coefficients, makes a recommendation for the rate coefficient at room temperature only with $k_1 = 5.5 \times 10^{-13} \text{ cm}^3 \text{ molecule}^{-1} \text{ s}^{-1}$ at 298 K.5 This number is reported to be associated with large uncertainty (58%), reflecting the scatter in individual determinations of k_1 . Rate coefficients derived using absolute methods vary from 1.1×10^{-12} cm³ molecule⁻¹ s⁻¹ (Dóbé et al. 1989) to $6.5 \times 10^{-13} \text{ cm}^3 \text{ molecule}^{-1} \text{ s}^{-1} \text{ (Scollard et al. 1993).}^{1,2} \text{ Relative}$ rate studies also report very different rate coefficients with values of 4.4×10^{-13} cm³ molecule⁻¹ s⁻¹ (Scollard *et al.* 1993), $4.8 \times 10^{-13} \ \mathrm{cm^3 \ molecule^{-1} \ s^{-1}}$ (Sellevåg 2004), $6.15 \times$ $10^{-13}~{\rm cm^3~molecule^{-1}~s^{-1}}$ and $6.93\times10^{-13}~{\rm cm^3~molecule^{-1}~s^{-1}}$ (Sulbaek-Andersen 2004). 2,3,22 These studies are discussed in detail in Section 3.2 where we compare them with our results.

For the equivalent non-fluorinated acetaldehyde (CH₃CHO) a negative temperature dependence for reaction with OH has been reported by Sivakumaran *et al.* 2003 and IUPAC over the temperature range 200–380 K.^{5,23} Literature studies have shown that the rate coefficient for OH with CH₃CHO is orders of magnitude larger than that for OH + CF₃CHO indicating a strong effect of the fluorine atoms on the reactions potential energy surface and thus its temperature dependence. The lack of published, temperature-dependent kinetic data for

OH + CF₃CHO thus makes prediction of its lifetime at various altitudes in the troposphere (where temperatures may vary between ~ 300 and 230 K) precarious and precludes accurate assessment of the lifetime of CF₃CHO and its potential to lead to TFA formation.

The objective of this research is to experimentally determine the temperature-dependent rate coefficient for the reaction of CF₃CHO with OH. To achieve this, we have used pulsed laser photolysis coupled with pulsed laser-induced fluorescence (PLP-PLIF) and online gas-phase FTIR measurements of reactant concentrations, which enable precise determination of rate coefficients across a large temperature range. Additionally, we conducted room-temperature relative-rate experiments in a photolytic reactor with *in situ* FTIR analysis (RR-FTIR).

2. Experimental

Absolute, temperature-dependent rate coefficients, $k_1(T)$, for the title reaction were obtained using pulsed laser photolytic (PLP) generation of OH coupled to pulsed laser induced fluorescence (PLIF) detection with [CF₃CHO] \gg [OH] (pseudofirst-order conditions). The concentration of CF₃CHO was measured *in situ via* Fourier-transform infra-red absorption (FTIR) spectroscopy. In further, relative-rate experiments using a photolytic chamber with FTIR absorption spectroscopy (RR-FTIR), the room temperature (298 \pm 2 K) rate coefficient was measured using C₂H₆ as reference reactant. The experimental setups are briefly described below; further details for the PLP-PLIF and RR-FTIR set-ups are found in Wollenhaupt *et al.* 2000 and Groß *et al.* 2014 (PLP-PLIF) and in Crowley *et al.* 1999 and Berasategui *et al.* 2020 (RR-FTIR).^{24–27}

2.1. PLP-PLIF experiments

Experiments were carried out in a double-jacketed quartz reactor (volume $\sim\!500~{\rm cm}^3)$ thermostatted by circulating ethanol (204 K to 300 K) or water (300 K to 364 K). The reactor is equipped with a K-type thermocouple, which was used to probe the temperature in the centre of the reactor (where the photolysis and excitation laser pulses overlap) before each experiment. The pressure in the reactor and FTIR-absorption cell (see below) was measured using 100 and 1000 Torr capacitance manometers. Gas flows were set up so that a linear velocity of $\sim\!70~{\rm cm~s^{-1}}$ was achieved, ensuring complete gas exchange for each photolysis pulse (10 Hz), preventing the accumulation of products. Gases were pre-mixed in a glass manifold before flowing into the reactor. A distance of $\sim\!15~{\rm cm}$ between the reactor inlet and the photolysis zone ensured a thermal equilibration with the reactor walls.

2.1.1. Generation of OH. Pulsed radiation for the *in situ* OH-radical generation from a suitable gas-phase precursor (see below) was provided by a KrF excimer laser (COMPex pro 201F, Coherent), which delivered pulses (\sim 20 ns) at 248 nm perpendicular to the gas flow direction. The laser fluence was measured with a Joule–meter positioned behind the exit window of the reactor and, based on the precursor absorption

cross-section and quantum yield at 248 nm, was used to calculate approximate, initial OH concentrations. A total of four schemes ((R6), (R7), (R8) + (R9), (R8) + (R10)) for generating OH were tested.

$$H_2O_2 + h\nu (248 \text{ nm}) \rightarrow 2 \text{ OH}$$
 (R6)

$$HNO_3 + h\nu (248 \text{ nm}) \rightarrow OH + NO_2$$
 (R7)

$$O_3 + h\nu (248 \text{ nm}) \rightarrow O(^1D) + O_2$$
 (R8)

$$O(^{1}D) + H_{2}O \rightarrow 2 OH$$
 (R9)

$$O(^{1}D) + CH_{4} \rightarrow OH + CH_{3}$$
 (R10)

Apart from photolysis of H_2O_2 all other schemes suffered from problems related to secondary chemistry or (for HNO₃) surface reaction with CF₃CHO. These issues are highlighted and discussed in the SI. All the PLP–PLIF rate coefficients we report were thus obtained using H_2O_2 as OH source, whereby typical H_2O_2 concentrations of $\sim 5 \times 10^{14}$ molecule cm⁻³ resulted in initial OH concentrations of $(1-5) \times 10^{10}$ molecule cm⁻³.

2.1.2. Detection of OH and CF₃**CHO.** OH radicals were excited (A² $\Sigma(\nu=1) \leftarrow X^2 \Pi$ ($\nu=0$) transition) at \sim 282 nm using a YAG-pumped dye laser (Quantel Brilliant B, Lambda Physik Scanmate). The subsequent OH fluorescence was detected using a photomultiplier screened by an interference filter (309 \pm 5 nm). The triggering of the photolysis and probe lasers was controlled by a digital delay generator. Transient OH profiles consisting of 20 pre-excimer pulses and 50 post-excimer pulses were obtained by accumulating the fluorescence signal using a boxcar averager. To achieve an improved signal-to-noise ratio, \sim 20 OH profiles were accumulated for the derivation of decay kinetics.

The CF₃CHO concentration was monitored by its infra-red absorption in a 45 cm long cell coupled to a FTIR spectrometer (Bruker-Vector 22 with an external, L_{N2}-cooled MCT detector). The absorption cell could be located either upstream or downstream of the reactor. Infrared absorption spectra were recorded with a resolution of 1 cm⁻¹ by coaddition of 64 interferograms (background: 128 interferograms) and phasecorrected and Boxcar-apodized (Mertz) with a zero-filling factor of 4. The measured CF₃CHO IR-absorbance was converted to a concentration by spectral deconvolution/fitting to a calibrated, CF₃CHO reference spectrum as well as other relevant absorbing species. There were no strong, unassigned bands in the spectrum and later we set upper limits to the concentrations of IRabsorbing impurities such as C₂H₄. The statistical uncertainty in the CF₃CHO concentration was generally <1% and always <3%. The CF₃CHO reference spectrum was obtained relative to the well-known UV-absorption spectrum of CF₃CHO by simultaneously recording optical density between 250 and 400 nm and absorbance in the 44 cm FTIR cell. For this purpose, the UVabsorption of CF₃CHO was measured in a multipass absorption cell with 880 cm optical path-length coupled to a UV-vis spectrometer with CCD-camera (Andor DU420A-OE).

The very good agreement in the absorption cross-section of CF₃CHO at λ_{max} = 300 nm between several studies (IUPAC: 3.06 \times 10⁻²⁰, Hashikawa 2006: 3.1 \times 10⁻²⁰, Chiappero 2006:

 2.92×10^{-20} , Meller 1993: 3.0×10^{-20} , Sellevag 2004: 3.17×10^{-20} in cm² molecule⁻¹) indicate that the uncertainty associated with the concentrations obtained in this manner (and thus the IR-cross-sections for CF₃CHO) are <5%. 3,5,28,29 Cross-sections obtained in independent experiments in which the IR absorption of CF₃CHO was determined using a short absorption cell (10 cm, with the CF₃CHO taken from the headspace of the pure liquid) were used to derive integrated band strengths that agreed to within 3% with those obtained when concentrations were derived by UV-absorption. These results are presented in detail in the SI.

2.2. Relative rate experiments, RR-FTIR

The relative rate experiments were carried out in a 44.39 L cylindrical quartz chamber equipped with *in situ*, infra-red analysis of CF₃CHO and the reference reactants. The same FTIR spectrometer was used as described in the PLP-PLIF experiments, in this case coupled to an internal, white-type multi pass mirror system resulting in an infra-red optical pathlength of 38.4 m. Infrared absorption spectra (600–3600 cm⁻¹) were recorded at 1 cm⁻¹ resolution by coaddition of between 64 and 128 interferograms.

Experiments were carried out on static samples at room temperature and a pressure of around 750 Torr using synthetic air or N_2 as bath gases. Gases (C_2H_6 , CF_3CHO , H_2 and O_3) were sequentially dosed via a glass vacuum line and flushed into the chamber with bath gas. The pressures in the chamber and the vacuum line were measured using capacitance manometers (reactor: 1000 mbar, vacuum line: 1000 mbar, 100 Torr, 10 Torr).

Photochemical OH generation was initiated by the photolysis of O_3 with eight radially-mounted, low-pressure Hg lamps providing a homogeneous light flux (~ 253.65 nm) in the chamber. O(1 D) was converted to OH via its reaction with H₂ as described previously.^{27,30}

$$O_3 + h\nu (253.65 \text{ nm}) \rightarrow O(^1D_2) + O_2$$
 (R11)

$$O(^{1}D_{2}) + H_{2} \rightarrow OH + H$$
 (R12)

$$H + O_2 + M \rightarrow HO_2 + M$$
 (R13)

Typically, initial concentrations of 1×10^{16} molecule cm⁻³ of O_3 and $0.5-2 \times 10^{17}$ molecule cm⁻³ of H_2 were used. The generation of OH in this manner also produces HO2 which further reacts (e.g. with O₃) to recycle OH.²⁷ Simulations of the chemistry indicate an [HO2]/[OH]0 ratio between 44 and 1900 depending on the initial H2 and O3 concentrations (see SI for further details). The use of H₂O₂ and HNO₃ as OH precursors was not possible in the relative-rate method as their rate coefficients for reaction with OH are much larger than for CF₃CHO. In addition, neither O3 nor H2 has strong absorption features in the relevant IR regions, which facilitates the analysis of the spectra. The initial concentrations of CF₃CHO and C₂H₆ were typically 8.5×10^{13} molecule cm⁻³ and 1.6×10^{14} molecule cm⁻³, respectively. As CF₃CHO absorbs dissociatively at 253.65 nm $(\sigma \sim 5 \times 10^{-21} \text{ cm}^2 \text{ molecule}^{-1})$, its slow loss due to photolysis needs to be taken into account for the relative-rate analysis.^{3,31} The first-order loss rate constant for CF₃CHO in this set-up (k_{phot})

Paper

was obtained by measuring its depletion in the chamber in different bath gases (N2, N2/H2 and synthetic air/H2) with the photolysis lamps on, but without adding O₃.

2.3. Chemicals

N₂ (Air Liquide, 99.999%) and synthetic air (Air Liquide, 99.999%) were used without further purification. Anhydrous HNO3 was prepared by mixing H₂SO₄ (Roth, 98%) and KNO₃ (Roth, >99%) and collecting the HNO₃ vapour in a liquid-nitrogen-cooled trap. The liquid HNO₃ was stored at −30 °C. H₂O₂ (AppliChem, 50 wt%) was concentrated by vacuum distillation to >90 wt%. H₂ (Westfalen, 99.999%) was used without further purification. O₃ was photochemically generated from O₂ (Westfalen, 99.999%) and stored on silica gel at -78 °C prior to each experiment. CF₃CHO was prepared by drying the monohydrate (Sigma Aldrich, 75% in water), passing it over P₂O₅ (Thermo Scientific, >99%) and collecting the vapour in a liquid-nitrogen-cooled trap. Diluted samples of gaseous CF₃CHO in N₂ (5-10 wt%) were prepared by manometric methods and stored in a darkened, 20 L glass bulb. C₂H₆ (Air Liquide, 99.95%) was used without further purification.

Results & discussion

3.1. Rate coefficients (204-364 K) for k_1 via PLP-PLIF

Fig. 1 displays a representative set of OH decays for a range of [CF₃CHO] obtained in N₂ bath gas at 296 K. The IR-absorbance by CF₃CHO for each [CF₃CHO] is shown in the lower panel of this Figure.

The time-dependent OH-LIF signals exhibit strictly monoexponential behaviour, characterized by their respective decay constants k'. Under pseudo-first-order conditions ([CF₃CHO] \gg [OH]₀), the time-dependent OH concentration [OH]_t is given by:

$$[OH]_t = [OH]_0 \times \exp(-k't) \tag{1}$$

where [OH]₀ is the initial concentration after the excimer-laser pulse. The first-order decay constant k' includes loss of OH due to reaction with CF₃CHO (k_1 [CF₃CHO]) as well as reaction with H₂O₂ and diffusive losses. As, for a given experiment, the pressure and temperature diffusive losses are constant and H₂O₂ is unchanged, the latter two terms can be combined as a single term d:

$$k' = k_1[CF_3CHO] + d (2)$$

The rate coefficient k_1 can thus be obtained by plotting k'versus [CF₃CHO] as shown in Fig. 2 for experiments conducted at different temperatures. As expected from (1), k' increases linearly with [CF $_3$ CHO]. The term d (the y-axis intercept) varied from one experiment to the next according to the temperature, pressure and the H₂O₂ concentration, with its values in the absence of CF₃CHO (not plotted) consistent with those derived from linear fits as shown in Fig. 2. All determinations of k_1 (a total of 17 at various temperatures), obtained using H₂O₂ photolysis as OH source, are listed in Table 1.

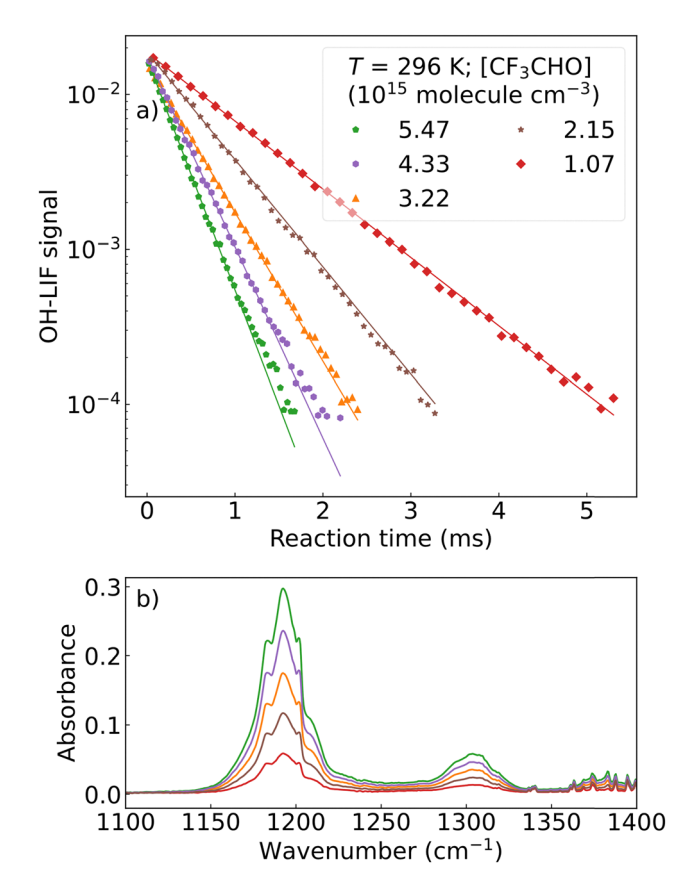


Fig. 1 (a) Exponential decay of the OH-LIF signal over two orders of magnitude versus reaction time for five different CF₃CHO concentrations at 296 K. H₂O₂ was used as photolytic OH source. (b) Corresponding FTIR spectra for the five different CF₃CHO concentrations recorded simultaneously with the PLP-PLIF measurements

As the rate coefficient for OH + CF₃CHO is not large, there is a potential for fast secondary reactions (i.e. reaction of OH with radical products) biasing the OH decay constant to high values. As an example, if we assume that CF₃CO radical product of the title reaction reacts with collision frequency (~ 2 × 10⁻¹⁰ cm³ molecule⁻¹ s⁻¹) with OH to form CF₃C(O)OH, then a ~0.1% conversion of CF₃CHO to CF₃CO would result in an enhancement of the OH decay rate (by up to a factor 2 at longer reaction times) and a distortion of the OH decay from monoexponential behaviour. Such secondary effects can be avoided by working at low initial OH concentrations and thus minimal conversion of CF₃CHO to reactive products. In our experiments the ratio of $[CF_3CHO]/[OH]_0$ was $>1 \times 10^4$ so such effects should be negligible. In order to confirm this, a series of experiments was conducted in which the laser fluence (and thus the initial OH concentration) was varied for a fixed H2O2 and CF_3CHO concentration. As shown in Fig. S2.1, k' was independent of the laser fluence and thus independent of [OH]₀ over the approximate range 1×10^{10} -5 $\times 10^{11}$ molecule cm⁻³. This confirms that reactions of OH with products did not influence our rate coefficients and also confirms that radical fragments formed in the photolysis of CF₃CHO did not play a significant role. This is to be expected as the absorption cross-section of

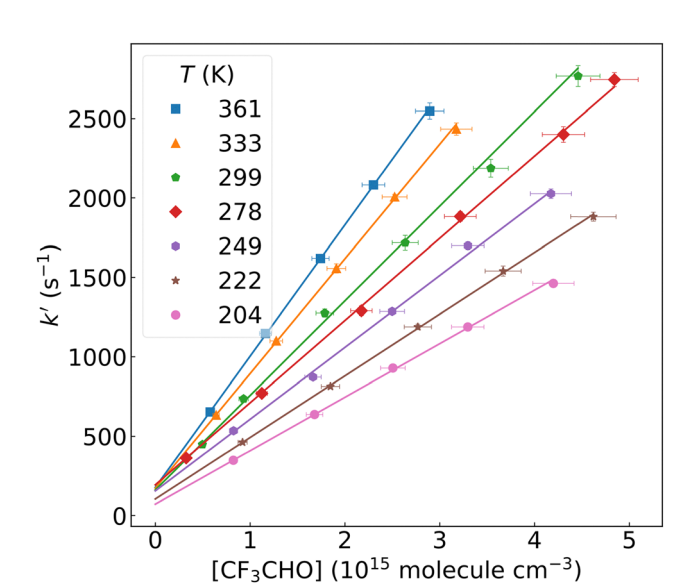


Fig. 2 OH decay constants k' versus the concentration of CF_3CHO at different temperatures. The y-axis intercept varies from 70 s⁻¹ to 190 s⁻¹ due to OH loss processes such as the reaction with H₂O₂. The horizontal error-bars combine the 2σ uncertainties obtained from spectral deconvolution, and an estimated systematic uncertainty of 5% related to the IRcross-section. Uncertainties in the decay constants k' correspond to the 2σ confidence intervals derived from mono-exponential fits to the OH-LIF signals

Table 1 Experimental rate coefficients k_1 obtained using PLP-PLIF

T (K)	p (Torr)	$k_1 (10^{-13} \text{ cm}^3 \text{ molecule}^{-1} \text{ s}^{-1})$	[CF ₃ CHO] (10 ¹⁵ molecule cm ⁻³)
204	103	3.4 ± 0.1	0.8-4.2
213	103	3.5 ± 0.2	1.0-3.8
222	103	3.9 ± 0.1	0.9-4.6
233	103	4.3 ± 0.1	0.8-4.0
244	104	4.0 ± 0.2	0.6-5.5
249	103	4.5 ± 0.3	0.8-4.2
268	96	4.8 ± 0.1	0.4-4.7
278	96	5.2 ± 0.1	0.3-4.8
283	97	5.3 ± 0.1	0.3-5.4
288	97	5.4 ± 0.2	0.3-5.1
294	108	5.6 ± 0.3	1.4-8.0
295	101	5.5 ± 0.1	1.4-5.4
296	107	5.6 ± 0.1	1.1-5.7
296	108	5.5 ± 0.1	1.1-5.5
299	104	6.0 ± 0.3	0.5-4.5
333	106	7.2 ± 0.1	0.6-3.2
361	106	8.3 ± 0.1	0.6-2.9

CF₃CHO at 248 nm $(2.60 \times 10^{-21} \text{ cm}^2 \text{ molecule}^{-1})$ is rather low.²⁹ The temperature dependent rate coefficients obtained are listed in Table 1 and also plotted in Fig. 3 where an overall positive dependence of k_1 on temperature is observed as well some curvature in the Arrhenius plot. The rate coefficients are well reproduced by the expression:

$$k_1(T) = (3.8 \pm 0.2) \times 10^{-13} \times (T/300)^2 \times \exp[(131 \pm 16)/T]$$
(3)

with all data within the 2σ confidence interval. The error bars represent statistical uncertainty only (2σ) as returned by weighted,

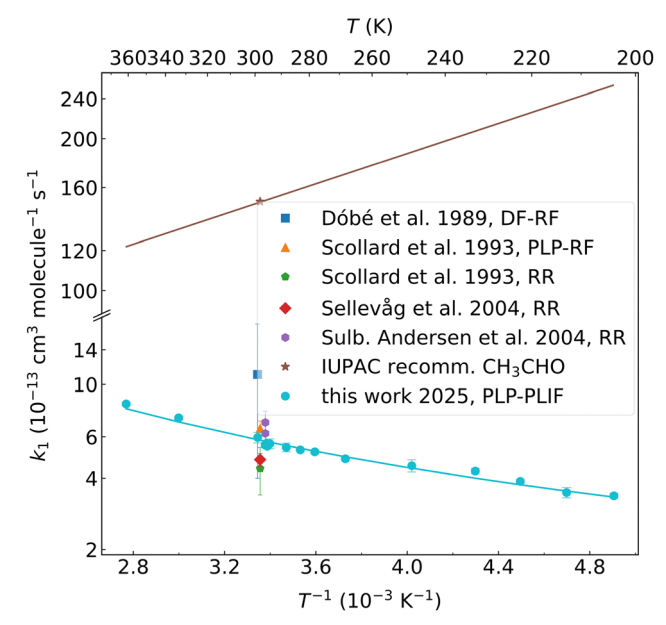


Fig. 3 Temperature dependent rate coefficients from this study (PLP-PLIF) along with literature values. $^{1-5}$ Uncertainties in k_1 correspond to the 2σ confidence interval derived from the linear fit of k' versus [CF₃CHO]. RR = relative rate method, DF-RF = discharge flow-resonancefluorescence method

least-squares fits to the data as shown in Fig. 2 and thus also include statistical uncertainty in deriving concentrations by leastsquares fitting of the FTIR spectra to a reference spectrum. A potential source of systematic bias in absolute rate coefficients is related to the measurement of the concentration of the excess reactant, i.e. CF3CHO. In this study, on-line measurement of [CF₃CHO] via IR absorption spectroscopy ensures that this parameter is known to better than 5% (see Section 2.1.3). A further potential source of error when measuring relatively low rate coefficients is the presence of reactive impurities which can lead to a positive bias. C₂H₄ is a known impurity in samples of CF₃CHO that reacts with OH $(k = 6.6 \times 10^{-12} \text{ cm}^3 \text{ molecule}^{-1} \text{ s}^{-1} \text{ at}$ 298 K and 100 Torr N₂). 32,33 C₂H₄ was indeed found as an impurity in our flowing CF₃CHO samples but at concentrations that were ≤0.1% of the CF₃CHO concentration. This would bias the result by $\sim 1\%$, which is much lower than our overall uncertainty and thus negligible.

Our rate coefficient at room temperature is a factor ~ 270 lower than the value of $1.5 \times 10^{-11} \text{ cm}^3 \text{ molecule}^{-1} \text{ s}^{-1}$ for the non-fluorinated analogue, CH3CHO.5

$$CH_3CHO + OH \rightarrow CH_3CO + H_2O$$
 (R14)

The positive dependence of k_1 on temperature also strongly contrasts k_{14} , which decreases with increasing temperature over the same range (i.e. from 2.6×10^{-11} at 205 K to $\sim 1.0 \times 10^{-11}$ at 355 K). As, in both cases, the reaction proceeds via abstraction of the aldehydic hydrogen atom, it is clearly the substitution of the CH₃ group by CF₃ that reduces the rate coefficient by reducing the electron density around the carbonyl group. In the case of CH₃CHO, OH is believed to form a pre-reaction complex

(PRC) with a five-membered ring in which the H-atom of OH is attached to the carbonyl oxygen.³⁴ From the PRC, the reaction may proceed via either passing over a barrier to products (i.e. a transition state in which the C-H bond lengthens compared to the PRC) or by tunnelling through the barrier, which leads to the observed negative dependence of $k(OH + CH_3CHO)$ on temperature. The lower electron density around the carbonyl group for CF₂CHO results in a much less stable PRC, for which the decomposition back to reactants is faster. This results in a reduced net flux through the transition state to products and thus to a lower rate constant. For CF₃CHO, the contribution of "direct" abstraction (with an associated positive dependence on temperature) becomes relatively more important. The different temperature dependencies observed for CF3CHO and CH₃CHO may also result from a difference in the barrier heights through the transition states relative to reactants.

3.2. Comparison with literature

The 298 K rate coefficient for the reaction of OH with CF₃CHO from this study is $5.8 \times 10^{-13} \text{ cm}^3 \text{ molecule}^{-1} \text{ s}^1 \text{ which can be}$ compared to room-temperature literature values, also plotted in Fig. 3. Our rate coefficient at 298 K agrees well with the IUPAC evaluation of previous datasets for this reaction.⁵ This agreement may however be somewhat fortuitous as the previous values cover a range of 1.1 \times 10⁻¹² to 4.4 \times 10⁻¹³ cm³ molecule $^{-1}$ s¹. The rate coefficient published by Scollard *et al.* was obtained by a similar method to that used here (pulsed laser photolysis to generate OH) and returned a value of k_1 = $6.5 \times 10^{-13} \ \text{cm}^3 \ \text{molecule}^{-1} \ \text{s}^1$ which is $\sim 12\%$ larger than our value.2 We note that Scollard et al. did not measure CF3CHO inline but relied on manometric measurements (i.e. partial pressures and partial flows) which are potential sources of systematic bias, and also do not discuss or rule out the presence of reactive impurities in their CF₃CHO samples (which were only stated to have >99% purity). In addition, the authors state that the initial CF₃CHO/OH ratio was greater than 100, which, given that they used a less sensitive technique for OH detection (resonance fluorescence rather than laser-induced-fluorescence), may not have been sufficient to rule out reactions of OH with secondary products. This in turn would have led to a high bias to their derived rate coefficient as described above. We cannot prove if any of these potential factors may have biased the Scollard et al. rate coefficient to slightly higher values than ours, but simply indicate that their slightly larger rate coefficient is consistent with such effects. Scollard et al. reported a value for k_1 at roomtemperature only, however the same experimental set-up was used to derive rate coefficients between 230 and 355 K, which were only reported as conference proceedings with $k_1 = 3.1 \times 10^{-5}$ $10^{-12} \exp[-(488 \pm 57)/T]$. As these data have not been rigorously peer-reviewed, the IUPAC panel has not considered them in their evaluations.⁵ The rate coefficients of Laverdet et al.³⁵ all lie \sim 10% higher than our values and the same potential reasons as described for Scollard et al. apply. In further absolute measurements of k1, Dóbé et al.1 used a low-pressure flow tube with resonance-fluorescence detection of OH at 299 K. In their experiments the CF₃CHO/OH ratio was between ~50 and 280 which

would almost certainly have biased their rate coefficients to high values. Indeed, their rate coefficient is the highest of all literature values ($k_1(299 \text{ K}) = 1.1 \times 10^{-12} \text{ cm}^3 \text{ molecule}^{-1} \text{ s}^1$) and was not considered by IUPAC in their evaluation.

In addition to the absolute studies, there are several relative rate experiments which report values of k_1 . As in the absolute studies, the values obtained also show considerable scatter (between (6.9 ± 0.1) and $(4.4 \pm 1.0) \times 10^{-13}$ cm³ molecule⁻¹ s⁻¹) depending on the choice of OH-source (RONO photolysis in air or O3 photolysis in the presence of H₂) and reference reactant including $CH_3C(O)CH_3$ ($k_{OH} = 1.8 \times 10^{-13} \text{ cm}^3 \text{ molecule}^{-1} \text{ s}^{-1}$), C_2H_6 ($k_{OH} = 2.4 \times 10^{-13} \text{ cm}^3 \text{ molecule}^{-1} \text{ s}^{-1}$), C_2H_4 ($k_{OH} = 7.8 \times 10^{-13} \text{ cm}^3 \text{ molecule}^{-1} \text{ s}^{-1}$) $10^{-12} \text{ cm}^3 \text{ molecule}^{-1} \text{ s}^{-1}$) and C_2H_2 ($k_{OH} = 7.5 \times 10^{-13} \text{ cm}^3$ molecule⁻¹ s⁻¹).⁵ With the exception of C_2H_4 , the other reference reactants all react with rate coefficients which are similar (within a factor of \sim two) to that of OH + CF₃CHO and are thus suitable for accurate determination of k_1 . The remaining three determinations yield rate coefficients (10⁻¹³ cm³ molecule⁻¹ s⁻¹) of 4.4 \pm 1.0 (Scollard *et al.* 1993), 4.8 \pm 0.3 and 5.44 \pm 0.71 (Sellevag et al. 2004), which are in reasonable agreement.^{2,3}

In order to better understand the differences between the various relative rate studies we conducted our own set of experiments in which the relative loss rates of CF_3CHO and C_2H_6 in the presence of an OH-source were determined.

3.3. Relative rate study of OH + CF₃CHO

The relative rate of reaction of OH with CF₃CHO (R1) and C₂H₆ (R15) was measured in the RR-FTIR set-up with the photolysis of O₃ providing the source of OH (R11).

$$C_2H_6 + OH \rightarrow products$$
 (R15)

As CF₃CHO is lost by both reaction with OH and photolysis the relative change in concentration of CF₃CHO and reference reactant is given by:

$$\ln\left(\frac{[\text{CF}_{3}\text{CHO}]_{0}}{[\text{CF}_{3}\text{CHO}]}\right) - J_{\text{phot}}t = \frac{k_{1}}{k_{15}} \times \ln\left(\frac{[\text{C}_{2}\text{H}_{6}]_{0}}{[\text{C}_{2}\text{H}_{6}]}\right)$$
(4)

where $[CF_3CHO]_0$ and $[C_2H_6]_0$ are initial concentrations of CF_3CHO and C_2H_6 , $[CF_3CHO]_t$ and $[C_2H_6]_t$ are the concentrations after reaction time t. k_1 and k_{15} are the bimolecular rate coefficients of the reaction of CF_3CHO and C_2H_6 with OH and $J_{\rm phot}$ is the photolysis frequency of CF_3CHO . $J_{\rm phot}$ = $(8.3 \pm 0.5) \times 10^{-5} \, {\rm s}^{-1}$ was determined by monitoring the depletion of CF_3CHO absorption features during the lights-on phase (but in the absence of O_3). More details are provided in the SI (Fig. S4.1).

In the relative-rate experiments, the relative change in concentration of both reactants was monitored *in situ* with FTIR using the infra-red absorption feature at 3030–2957 cm⁻¹ for C_2H_6 and three different features of CF_3CHO at 1335–1280 cm⁻¹, 1210–1165 cm⁻¹ and 840–860 cm⁻¹. Exemplary FTIR spectra at reaction times of 0, 40 and 170 s are displayed in Fig. 4 along with reference spectra for CF_3CHO and C_2H_6 . The strong absorption feature at around 2100 cm⁻¹ is from O_3 . The spectra were baseline corrected and the absorption

PCCP Paper

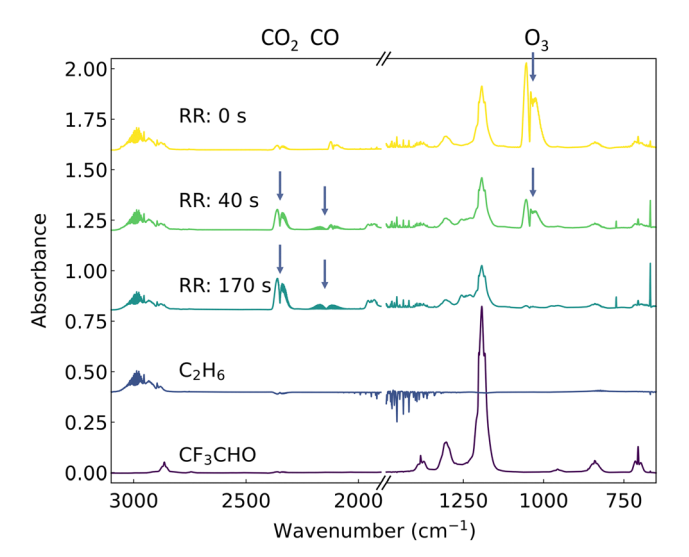


Fig. 4 Plot of the FTIR-spectra measured during a relative-rate experiment at different reaction times (0 s, 40 s and 170 s, upper three traces) along with reference spectra of C_2H_6 and CF_3CHO . The sharp features around 1800 cm⁻¹ are due to H₂O vapour. The traces have been vertically offset for clarity of display.

features of H₂O were removed as far as possible by fitting the spectra (2100-1300 cm⁻¹) to a reference spectrum of H₂O. In each composite spectrum, the concentrations of CF₃CHO and C₂H₆ were extracted by orthogonal distance regression to the reference spectra and also the spectra of any overlapping products that could be identified during the experiments. Since all the absorption features used exhibited Beer-Lambert linearity over the concentration range studied (see Fig. S1.2), the ratio of the fitting coefficients is equivalent to the concentration ratio, i.e. $[CF_3CHO]_0/[CF_3CHO]_t$ and $[C_2H_6]_0/[C_2H_6]_t$.

As is apparent from Fig. 4, the concentration of O₃ decreases very rapidly, which is related to not only its photolysis but also secondary reactions with H-atoms and both OH and HO2 radicals (see the SI for more details of the chemical scheme). Both CO₂ and CO (absorption features at ~2350 and 2140 cm⁻¹) are clearly observed products from the degradation of the organic reactants.

Fig. 5 displays the depletion factors for CF₃CHO and C₂H₆, the slope of which gives the relative rate coefficient (k_1/k_{15}) for an experiment conducted with 1.1×10^{16} molecule cm⁻³ of H₂. As discussed previously by Sellevåg et al., H2 serves two purposes; converting O(1D) to OH and also scavenging CF₃O in order to prevent it from reacting with either CF₃CHO or C₂H₆.³

Values of (k_1/k_{15}) obtained using the relative-rate method range from (1.39 \pm 0.03) to (3.06 \pm 0.09) depending on the experimental conditions (see Table 2). Using the IUPACrecommended rate coefficient for OH + C_2H_6 ($k_{15} = 2.4 \times 10^{-13}$ molecule cm⁻³), the rate coefficient for CF₃CHO + OH varies between (3.3 \pm 0.3) to (7.4 \pm 0.7) \times 10⁻¹³ cm³ molecule⁻¹ s^{-1.5} The variation in the rate coefficient is attributed to (1) the formation of CF₃O radicals and their reaction with CF₃CHO or C₂H₆ when [H₂] is low ((R16) and (R17)) and (2) the removal of CF₃CHO via reaction with HO₂ (R18), when [H₂] is high.³⁶

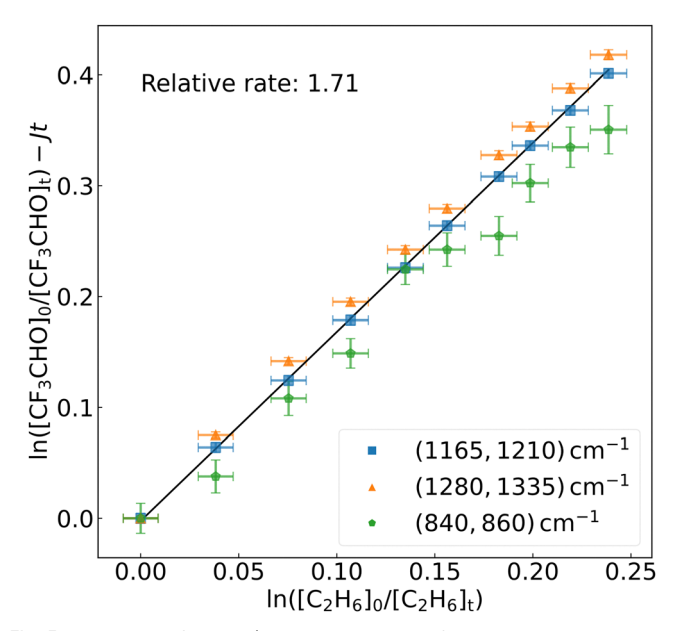


Fig. 5 Depletion factors (logarithmic ratio of initial concentration to concentration at reaction time t) for CF₃CHO and C₂H₆ obtained in a relative-rate experiment in N_2 with 1.1×10^{16} molecule cm⁻³ of H_2 . The CF_zCHO depletion factor contains the term Jt which takes into account its slow loss owing to photolysis. The different colours represent different IRabsorption features that were used to derive the depletion of CF₃CHO and the linear fit (black line) represents an average.

Table 2 Summary of relative rate experiments

Relative rate ^a	Absolute k_1^b (cm ³ molecule ⁻¹ s ⁻¹)	Initial $[H_2]$ (molecule cm ⁻³)	Bath gas
1.39 ± 0.03 1.30 ± 0.03 1.71 ± 0.04 1.95 ± 0.10 3.07 ± 0.09	$\begin{array}{l} (3.3\pm0.3)\times10^{-13} \\ (3.1\pm0.3)\times10^{-13} \\ (4.1\pm0.4)\times10^{-13} \\ (4.7\pm0.5)\times10^{-13} \\ (7.4\pm0.7)\times10^{-13} \end{array}$	4.3×10^{15} 1.1×10^{16} 1.1×10^{16} 1.4×10^{17} 1.9×10^{17}	Air Air N ₂ Air Air

^a $k(OH + CF_3CHO)/k(OH + C_2H_6)$. ^b Based on $k(OH + C_2H_6) = 2.4 \times 10^{-6}$ 10^{-13} cm³ molecule⁻¹ s⁻¹.

$$CF_3O + CF_3CHO \rightarrow CF_3CO + CF_3OH$$
 (R16)

$$CF_3O + C_2H_6 \rightarrow C_2H_5 + CF_3OH$$
 (R17)

$$CF_3O + H_2 (+ O_2) \rightarrow HO_2 + CF_3OH$$
 (R18)

The source of the CF₃O radicals in these experiments is secondary reactions of CF_3O_2 , themselves formed in e.g. the self-reaction of the CF₃C(O)O₂ radical. The rate coefficient for the reaction of CF₃O with C_2H_6 is 1.3×10^{-12} cm³ molecule⁻¹ s⁻¹ but the rate coefficient for CF_3O with $CF_3CHO(k_{16})$ is not known.⁵ The rate coefficient k_{16} was therefore estimated by assuming the same rate coefficient ratio of k(OH + CF₃CHO)/k(CF₃O + CF₃CHO) as that for $k(OH + C_2H_6)/k(CF_3O + C_2H_6)$, resulting in $k_{16} = 3 \times 10^{-12} \text{ cm}^3$ molecule⁻¹ s⁻¹. In a similar manner, by analogy with the rate coefficients for OH with H2 and CH4, the rate coefficient for the reaction of CF₃O with H₂ was estimated to be 2×10^{-12} cm³ molecule⁻¹ s⁻¹. A concentration of H_2 of 2.3×10^{16} molecule cm⁻³

Table 3 Key reactions considered in the numerical simulations

Reaction	k(298 K) (cm ³ molecule ⁻¹ s ⁻¹)
OH reactions OH + CF ₃ CHO → H ₂ O + CF ₃ CO	5.8×10^{-13}
$OH + C_2H_6 \rightarrow H_2O + CH_2CH_3$ $OH + C_2H_6 \rightarrow H_2O + CH_2CH_3$	$2.4 \times 10^{-13} (\text{IUPAC})^5$
Photolysis of TFAA $CF_3CHO \rightarrow CF_3 + HCO$ $CF_3CHO \rightarrow CF_3H + CO$	$\begin{array}{l} 3.28 \times 10^{-5} \; s^{-1} \; (IUPAC)^5 \\ 3.04 \times 10^{-5} \; s^{-1} \; (IUPAC)^5 \end{array}$
CF ₃ O reactions: CF ₃ O + CF ₃ CHO \rightarrow CF ₃ OH + CF ₃ CO CF ₃ O + C ₂ H ₆ \rightarrow CF ₃ OH + CH ₂ CH ₃ CF ₃ O + H ₂ \rightarrow CF ₃ OH + H	3.0×10^{-12} (Assumed) 1.3×10^{-12} (IUPAC) ⁵ 2.0×10^{-12} (Assumed)
HO_2 reactions $HO_2 + CF_3CHO \rightarrow CF_3CH(O)HOO$ $CF_3CH(O)HOO \rightarrow HO_2 + CF_3CHO$ $CF_3CH(O)HOO + HO_2 \rightarrow$ $CF_3CH(OH)OOH + O_2$	2.3×10^{-13} (Long et al., 2022) ³⁶ 2.0×10^{3} (Long et al., 2022) ³⁶ 1.0×10^{-11} (Assumed)

is thus needed to reduce the loss of C_2H_6 and CF_3CHO with CF_3O to <1% of their total (OH-dominated) loss.

To assess the impact of these reactions, we carried out numerical simulations of the chemistry (FACSIMILE³⁷) using an assumed reaction scheme (see Table S5.1). The key reactions in the scheme are listed in Table 3. Increasing the H_2 concentration reduces the potential impact of the unwanted reactions of CF_3O with CF_3CHO and C_2H_6 so one would expect the experiments at the highest H_2 concentrations to result in more accurate results. However, the use of very high H_2 also means that not only the CF_3O radical but also a significant fraction of the initially formed OH reacts with H_2 (in air) to form the HO_2 radical ((R19) and (R20)).

$$OH + H_2 \rightarrow H_2O + H \tag{R19}$$

$$H + O_2 + M \rightarrow HO_2 + M \tag{R20}$$

The use of high concentrations of $\rm H_2$ thus results in a shift in the $[\rm HO_2]/[\rm OH]_0$ ratio towards $\rm HO_2$ with the simulated ratios varying from 47 at $[\rm H_2]$ = 10^{16} molecule cm⁻³ to 789 at $[\rm H_2]$ = 2 × 10^{17} molecule cm⁻³ ($[\rm O_3]$ = 10^{16} molecule cm⁻³). According to a theoretical study, ³⁶ the $\rm HO_2$ radical may react with CF₃CHO to form the CF₃CH(OH)OO peroxy radical (R21) with a rate coefficient of k_{20} = 2.34×10^{-13} cm³ molecule⁻¹ s⁻¹.

$$CF_3CHO + HO_2 \rightarrow CF_3CH(OH)OO$$
 (R21)

$$CF_3CH(OH)OO \rightarrow CF_3CHO + HO_2$$
 (R22)

CF₃CH(OH)OO is unstable at room temperature and decomposes back to reactants on a ms timescale (k_{21} = 1.72 × 10³ s⁻¹), which reduces the impact of the reaction between HO₂ with CF₃CHO (R22). However, given the high radical densities in these experiments, some fraction of the CF₃CH(OH)OO radical may react with OH or HO₂ ((R23) and (R24)). This would bias the relative rate coefficient to high values by providing an unwanted, extra sink of CF₃CHO.

$$CF_3CH(OH)OO + OH \rightarrow products$$
 (R23)

$$CF_3CH(OH)OO + HO_2 \rightarrow products$$
 (R24)

The rate coefficients for (R23) and (R24) are unknown, but a reasonable estimate can be obtained by drawing analogy to other $HO_2 + RO_2$ ($k \sim 1 \times 10^{-11}$ cm³ molecule⁻¹ s⁻¹) and OH + RO_2 reactions ($k \sim 1 \times 10^{-10}$ cm³ molecule⁻¹ s⁻¹).

Using the theoretical rate coefficients from Long et al. 36 for the reactions (R20) and (R21) and the estimated rate coefficients for CF₃O with CF₃CHO and H₂, the results of the numerical simulations (see SI for a detailed discussion and Figures) show that, as observed, the relative rate coefficient obtained in the O₃/ H₂ photolysis system suffer from systematic bias owing to unwanted reactions of CF₃O with both reactants (when [H₂] is too low) and also reactions of HO₂ with CF₃CHO (when [H₂] is too large). There thus appears to be a narrow window of H₂ concentrations in which these biases in the relative-rate measurements are minimised, and the value obtained approaches that derived from the PLP-PLIF experiments. We conclude that the relative rate studies of this reaction using the OH generation scheme outlined are unlikely to lead to accurate results for k_1 . We note that the use of other OH source in relative rate experiments (e.g. the photolysis of CH₃ONO/NO mixtures) could conceivably deliver accurate rate coefficients if sufficient NO (or CH3ONO) is present to scavenge any CF₃O formed and thus prevent its reaction with CF₃CHO or the chosen reference reactant. Such experiments were carried out by Sulbaek-Andersen et al. and Scollard et al., though the authors did not consider the possible interfering role of CF₃O.^{2,22} In the experiments of Sulbaek-Andersen et al., a large concentration of CH₃ONO was used (a factor 5-10 more than CF₃CHO) which may plausibly have been sufficient to scavenge most CF₃O. In contrast, Scollard et al. used almost identical amounts and it is not possible to rule out that some loss of CF₃CHO and/or reference reactant biased their results. The excellent agreement between our PLP-PLIF rate coefficient at room temperature and that obtained by Sulbaek-Andersen et al. using the relative-rate technique likely reflects avoidance of potential pitfalls when determining k_1 using absolute and relative methods.

4. Conclusions and atmospheric lifetime of CF₃CHO

We have investigated the reaction between OH and CF₃CHO using PLP-PLIF over an atmospherically relevant temperature range of 204 K to 361 K using a number of OH sources whereby only the photolysis of H_2O_2 generated reproducible, accurate rate coefficients. Our results are summarised by the expression $k_1(T) = (3.8 \pm 0.2) \times 10^{-13} \times (T/300)^2 \times \exp[(131 \pm 16)/T] \text{ cm}^3$ molecule⁻¹ s⁻¹, reflecting a weak positive dependence on temperature over this temperature range. This is the opposite trend to that observed for the non-fluorinated analogue which, (along with the much lower absolute values of the rate coefficient) is related to destabilisation of the pre-reaction complex by the substitution of H- with F-atoms on the methyl-group. A

series of relative rate experiments revealed sources of potential bias involving formation of the CF₃O radical and its reaction with CF₃CHO and the reference reactant, as well as reactive loss of CF₃CHO through reaction with the HO₂ radical.

For the reasons listed above, we consider our PLP-PLIF experiments, conducted using very high [CF₃CHO]/[OH]₀ ratios and also better control of impurities, to be more reliable than the previously published absolute rate studies, which were conducted at room-temperature only. In addition, our room temperature result $(k_1 = (5.8 \pm 0.5) \times 10^{-13} \text{ cm}^3 \text{ molecule}^{-1} \text{ s}^{-1})$ is in excellent agreement with the previous relative rate study by Sulbaek-Andersen et al. $(k_1 = (5.4 \pm 0.7) \times 10^{-13} \text{ cm}^3 \text{ molecule}^{-1} \text{ s}^{-1})$, which is likely the least affected by secondary reactions involving the CF₃O radical.²² The tropospheric lifetime of CF₃CHO with respect to OH can be estimated using our temperature dependent rate coefficient and an approximate OH concentration (independent of altitude) of 10⁶ molecule cm⁻³. Based on a standard temperature profile,³⁸ the lifetime in the lower three kilometres of the troposphere is estimated to be 22 days, increasing to 30 days at altitudes between 8 and 11 kilometres due to the lower temperatures. This is longer than the CF₃CHO lifetime with respect to photolysis, which is presently thought to be <1 week in the boundary layer for which photolysis quantum yields close to room temperature are available.5

Conflicts of interest

There are no conflicts to declare.

Data availability

IR characterization of reactants, additional details on the measurements (PLP-PLIF and RR-FTIR), and simulations (reaction scheme) supporting this article are included in the SI. See DOI: https://doi.org/10.1039/d5cp02871j

Acknowledgements

The authors thank AstraZeneca for partial financial support of this investigation. Open Access funding provided by the Max Planck Society.

References

- 1 S. Dóbé, L. A. Khachatryan and T. Bérces, Z. Phys. Chem., 1989, 93, 847.
- 2 D. J. Scollard, J. J. Treacy, H. W. Sidebottom, C. Balestra-Garcia, G. Laverdet, G. Lebras, H. Macleod and S. Teton, J. Phys. Chem., 1993, 97, 4683.
- 3 S. R. Sellevåg, T. Kelly, H. Sidebottom and C. J. Nielsen, Phys. Chem. Chem. Phys., 2004, 6, 1243.
- 4 M. P. Sulbaek Andersen, C. Stenby, O. J. Nielsen, M. D. Hurley, J. C. Ball, T. J. Wallington, J. W. Martin, D. A. Ellis and S. A. Mabury, J. Phys. Chem. A, 2004, 108, 6325.

- 5 M. Ammann, R. A. Cox, J. N. Crowley, H. Herrmann, M. E. Jenkin, V. F. McNeill, A. Mellouki, M. J. Rossi, J. Troe and T. J. Wallington, Evaluated kinetic and photochemical data for atmospheric chemistry, 2025, https://iupac.aeris-data.fr/.
- 6 J. C. Boutonnet, P. Bingham, D. Calamari, C. D. Rooij, J. Franklin, T. Kawano, J.-M. Libre, A. McCul-loch, G. Malinverno, J. M. Odom, G. M. Rusch, K. Smythe, I. Sobolev, R. Thompson and J. M. Tiedje, Hum. Ecol. Risk Assess., 1999, 5, 59.
- 7 K. R. Solomon, G. J. M. Velders, S. R. Wilson, S. Madronich, J. Longstreth and P. J. Aucamp, J. Toxicol. Environ. Health, Part B, 2016, 19, 289.
- 8 R. Britton, V. Gouverneur, J.-H. Lin, M. Meanwell, C. Ni, G. Pupo, J.-C. Xiao and J. Hu, Nat. Rev. Methods Primers, 2021, 1, 47.
- 9 S. Caron, Org. Process Res. Dev., 2020, 24, 470.
- 10 Y. Ogawa, E. Tokunaga, O. Kobayashi, K. Hirai and N. Shibata, iScience, 2020, 23, 101467.
- 11 M. S. Javadi, R. Søndergaard, O. J. Nielsen, M. D. Hurley and T. J. Wallington, Atmos. Chem. Phys., 2008, 8, 3141.
- 12 M. D. Hurley, T. J. Wallington, M. P. Sulbaek Andersen, D. A. Ellis, J. W. Martin and S. A. Mabury, J. Phys. Chem. A, 2004, 108, 1973.
- 13 W. M. O. (WMO), State of the Global Climate 2022, Geneva, 2023.
- 14 J. B. Burkholder, R. A. Cox and A. R. Ravishankara, Chem. Rev., 2015, 115, 3704.
- 15 T. J. Wallington, M. P. S. Andersen and O. J. Nielsen, Adv. Atmos. Chem., 2017, 305, DOI: 10.1142/9789813147355 0005.
- 16 X. Zhang and Y. Li, Energy, 2024, 311, 133423.
- 17 A. Tewari, A. Parashar, W. Ahmad, A. Kumar, R. K. Vishwkarma, M. A. Ansari and P. Argulles, Compressors and Blowers: Maintenance, Practical Guidance, Energy-Efficient Technologies, 2025, 13, 179.
- 18 Y. Wang, Z. Wang, M. Sun, J. Guo and J. Zhang, Sci. Total Environ., 2021, 780, 146631.
- 19 M. P. Pérez-Peña, J. A. Fisher, C. Hansen and S. H. Kable, Environ. Sci.: Atmos., 2023, 3, 1767.
- 20 M. L. Hanson, S. Madronich, K. Solomon, M. P. Sulbaek Andersen and T. J. Wallington, Environ. Toxicol. Chem., 2024, 43, 2091.
- 21 J. Salas, A. L. Cardona, M. A. Burgos Paci and F. E. Malanca, Atmos. Environ., 2024, 337, 120780.
- 22 M. P. Sulbaek Andersen, O. J. Nielsen, M. D. Hurley, J. C. Ball, T. J. Wallington, J. E. Stevens, J. W. Martin, D. A. Ellis and S. A. Mabury, J. Phys. Chem. A, 2004, 108, 5189.
- 23 V. Sivakumaran and J. N. Crowley, Phys. Chem. Chem. Phys., 2003, 5, 106.
- 24 M. Wollenhaupt, S. A. Carl, A. Horowitz and J. N. Crowley, J. Phys. Chem., 2000, 104, 2695.
- 25 C. B. M. Groß, T. J. Dillon, G. Schuster, J. Lelieveld and J. N. Crowley, J. Phys. Chem. A, 2014, 118, 974.
- 26 J. N. Crowley, G. Saueressig, P. Bergamaschi, H. Fischer and G. W. Harris, Chem. Phys. Lett., 1999, 303, 268.
- 27 M. Berasategui, D. Amedro, A. Edtbauer, J. Williams, J. Lelieveld and J. N. Crowley, Atmos. Chem. Phys., 2020, 20, 2695.

Paper

28 R. Atkinson, D. L. Baulch, R. A. Cox, J. N. Crowley, R. F. Hampson, R. G. Hynes, M. E. Jenkin, M. J. Rossi, J. Troe and T. J. Wallington, *Atmos. Chem. Phys.*, 2008, **8**, 4144.

- 29 M. S. Chiappero, F. E. Malanca, G. A. Argüello, S. T. Wooldridge, M. D. Hurley, J. C. Ball, T. J. Wallington, R. L. Waterland and R. C. Buck, J. Phys. Chem. A, 2006, 110, 11944.
- 30 A. J. C. Bunkan, G. Srinivasulu, D. Amedro, L. Vereecken, T. J. Wallington and J. N. Crowley, *Phys. Chem. Chem. Phys.*, 2018, 20, 11306.
- 31 Y. Hashikawa, M. Kawasaki, R. L. Waterland, M. D. Hurley, J. C. Ball, T. J. Wallington, M. P. S. Andersen and O. J. Nielsen, *J. Fluorine Chem.*, 2004, **125**, 1925.
- 32 R. Atkinson, D. L. Baulch, R. A. Cox, J. N. Crowley, R. F. Hampson, R. G. Hynes, M. E. Jenkin, M. J. Rossi and J. Troe, *Atmos. Chem. Phys.*, 2006, 3625, DOI: 10.5194/acp-6-3625-2006.

- 33 M. P. Sulbaek Andersen, M. D. Hurley, T. J. Wallington, J. C. Ball, J. W. Martin, D. A. Ellis, S. A. Mabury and O. J. Nielsen, *Chem. Phys. Lett.*, 2003, 379, 28.
- 34 I. W. M. Smith and A. R. Ravishankara, J. Phys. Chem. A, 2002, 106, 4798.
- 35 G. Laverdet, G. Le Bras, H. MacLeod, G. Poulet, S. Teton, D. Scollard, J. Treacy and H. Sidebottom, *Laser photolysis-resonance fluorescence investigation of the reactions of hydro-xyl radicals with CCl3CHO and CF3CHO as a function of temperature*, SPIE, 1993.
- 36 B. Long, Y. Xia and D. G. Truhlar, *J. Am. Chem. Soc.*, 2022, 144, 19910.
- 37 A. R. Curtis and W. P. Sweetenham, Facsimile, Atomic Energy Research Establishment, Report R-12805, 1987.
- 38 U. S. Atmosphere, *US standard atmosphere*, National Oceanic and Atmospheric Administration, 1976.